Journal of Thermal Analysis and Calorimetry, Vol. 71 (2003) 883–892

DISTINGUISHING BETWEEN NATURAL AND RECARBONATED CALCITE IN OIL SHALE ASHES

S. Shoval[1*], *O. Yofe*[2] *and Y. Nathan*[2]

[1]Department of Natural Sciences, The Open University of Israel, 16, Klausner St., 61392 Tel Aviv, Israel
[2]Geological Survey of Israel, 30, Malkhei Israel St., 90550 Jerusalem, Israel

Abstract

Oil shale ashes from the PAMA demonstration power plant in the Negev region of Israel are produced by fluidized bed combustion (700–850°C) under short residence time. The FED is organic-rich calcareous raw material rich in carbonate rather than clays. Thus it is important to ascertain whether the calcite in the ashes is original natural calcite from the raw material or the product of recarbonation of lime. Three groups of ashes from the power plant, Ash Cooler (AC), Fly Ash (FAS) and Boiler Bank (BB) were examined using XRD, FT-IR, SEM and isotope analysis methods. The recarbonated calcite is distinguished from the natural original by smaller crystal size, lower degree of crystallinity and the presence of impurities. High negative $\delta^{13}C$ values in oil shale ashes are explained by assuming recarbonation of lime with CO_2 originating from the combustion of the organic matter of the raw oil shale. Fly Ash, FAS, and BB, produced from organically-rich FED, contain more recarbonated calcite than bottom ash, AC. This observation can be explained by the larger grains of the AC, which do not reach the highest temperature area, and thus most of the original calcite does not decompose.

Keywords: ash, calcite, decarbonation, lime, oil shale, recarbonation

Introduction

The thermal decarbonation of calcite has been intensively studied [1]. Upon firing the calcareous raw material to temperatures of about 700–850°C, carbon dioxide gas (CO_2) is released from the original calcite, and calcium oxide (CaO) is formed. In DTA experiments, the endothermic peak of the decarbonation process of crystalline calcite appears only at about 900°C due to the rapid rate of heating [1, 2]. Under prolonged heating; the temperature of decarbonation depends on the duration of heating, the crystal size and crystallinity of the original calcite, and the presence of impurities [3]. The presence of clay reduces the temperature of decarbonation [4–7]. In the presence of clay, under prolonged heating (6 h), the decarbonation process is completed at about 750°C in mono-

* Author for correspondence: E-mail: shoval@openu.ac.il

1388–6150/2003/ $ 20.00

Akadémiai Kiadó, Budapest
Kluwer Academic Publishers, Dordrecht

crystalline calcite, at about 650°C in spary calcite (sparite) of limestone, and at about 600°C in microcrystalline calcite (micrite) of chalk [3].

After firing, in ambient conditions the hygroscopic lime (CaO) picks up moisture from the air, forming calcium hydroxide [$Ca(OH)_2$] [1]. The recarbonated calcite is slowly formed by the reaction of the $Ca(OH)_2$ with atmospheric CO_2 [3, 7]. Some calcite is recarbonated during cooling [2]. Recarbonated calcite usually crystallizes with small crystal size and a low degree of crystallinity [8, 9]. In firing calcareous clay above 900°C, the free lime reacts with the thermal products resulting from the dehydroxylation of clays [6, 7]. As a result, Ca-silicates are formed [10–12]. This reaction reduces the amount of free lime and thus the amount of recarbonated calcite.

The PAMA demonstration power plant is located in Mishor Rotem, near the largest oil shale body known in the Negev of Israel. It is operated by fluidized bed combustion in the boiler of the plant. An open pit, the Havarbar mine, has been developed to supply raw material. The FED is mainly organic-rich 'bituminous' sediment of the Maastrichtian Ghareb Formation, traditionally termed 'oil shale', although the inorganic fraction is dominated by carbonate rather than clays [13]. The mineralogy of PAMA oil shale ashes is different from that of thermal products obtained in laboratory experiments and conventional kilns [14, 15]. The ashes contain a large amount of amorphous Ca-silicates, together with anhydrite, calcite and lime. The mineralogical differences are due to the much shorter residence time in the hottest part of the boiler in the fluidized bed.

The aim of this paper is to distinguish between natural and recarbonated calcite within the oil shale ashes and to follow the process of decarbonation during a short residence time. Differentiating between original and recarbonated calcite helps to understand and optimize the combustion. The amount of recarbonated calcite together with the remaining 'free' CaO (lime) gives the original amount of lime produced during combustion. Since it is important to produce as little lime as possible, estimation the amount of recarbonated calcite is essential.

Samples

Calcareous raw oil shale (FED) and three groups of oil shale ashes: Ash Cooler (AC), Fly Ash (FAS) and Boiler Bank (BB) from the PAMA demonstration power plant in the Negev were examined [15]. The fluidized bed combustion of organic-rich FED took place at 700–850°C under short residence time, less than one minute. The coarse-grained (1–8 mm) bottom ash, AC, is exposed to the lowest temperatures and to the longest residence time in the boiler, compared to the light-grained (0.1–1 mm) FAS and BB, which are exposed to higher temperatures under much shorter residence times.

Methods

X-ray diffractometry (XRD): acquired on powder samples with a Philips PW-1820 diffractometer using CuK_α radiation 35 kV–40 mA, and a curved graphite monochromator.

Infrared spectroscopy (FT-IR): obtained using a Nicolet FT-IR spectrometer and 'Omnic' software. KBr disks were employed. The disks were heated to 110°C to remove water bands. Immediately after heating, the disks were re-pressed (without regrinding) to improve the resolution of the spectra.

Scanning electron microscopy (SEM): was performed using a JEOL (JSM-840) instrument. The samples were examined mainly as dispersed powders. Point chemical analyses of discrete samples were carried out with an attached LINK 1000 EDS (Oxford ISIS). Calculations utilized the ZAF4/FLS program.

Isotope analysis: Stable isotope compositions of carbon and oxygen of the calcite were analyzed by VG SIRA-II Mass Spectrometer. The results obtained in selected ashes were compared to analyses of raw oil shale.

Curve fitting: The infrared spectra were analyzed using the Peak fitting function in 'Grams' software (Galactic Industries Corporation). A Lorentzian shape was used for fitting sharp components and a Gaussian shape for fitting broad components. Multiple points on either side of the region of interest were used for baseline linearization. Frequencies, widths and areas of the bands were calculated by the software for best fit.

Results and discussion

X-ray diffractometry

Table 1 summarizes the mineral composition of the Negev oil shales and of the FED according to XRD [14]. The FED is organic-rich calcareous raw material rich in carbonate rather than clays. X-ray diffractograms of the three ashes are shown in Fig. 1. The diffractograms demonstrate the presence of calcite, lime, anhydrite, and some

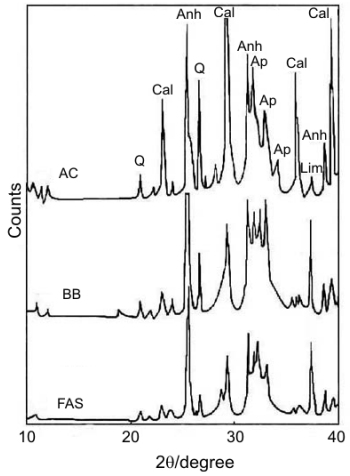

Fig. 1 X-ray diffractograms of AC, FAS and BB ashes produced from organically-rich FED. The diffractograms demonstrate the presence of calcite (Cal), lime (Lim), anhydrite (Anh) and some apatite (Ap) and quartz (Q)

apatite and quartz. It should be noted that XRD is not sensitive to amorphous phases of Ca-silicates and to the meta-clay observed by FT-IR spectroscopy. Sharp and strong diffraction peaks of calcite and small diffraction peaks of lime characterize the AC. The diffractions of the calcite are similar to those observed in the original calcite of the FED, indicating that in the AC, most of the calcite is original. On the other hand, small asymmetric diffraction peaks of calcite and strong diffraction peaks of lime characterize the BB and FAS produced from organically-rich FED. The strong diffraction peaks of lime indicate that the original calcite was decarbonated during combustion. It seems that the small asymmetric diffraction peaks of calcite in the BB and FAS are of initial recarbonated calcite. The broadening and asymmetry of the diffraction peaks of the recarbonated calcite are in accordance with small crystal size and low crystallinity, typical of recarbonated calcite [8, 9]. The calcite in AC is much better crystallized than in FAS and has a higher concentration.

Table 1 The mineral composition (in %) of the Negev oil shales and of the FED according to XRD

Minerals	Negev oil shales	FED
Organic matter	10–22	>12
Calcite	40–65	>40
Clay minerals*	5–25	>10
Apatite	4–10	<10
Quartz	<5	<5
Gypsum	<5	<5
Pyrite	<2	<2

*Kaolinite, smectite, illite and mixed layers

FT-IR spectroscopy

FT-IR spectra of the FED and the three ashes are shown in Fig. 2. The spectra demonstrate the presence of lime, calcite, anhydrite, meta-clay and amorphous Ca-silicates [15]. Frequencies (cm^{-1}) and relative intensities of the principal bands of these phases in FT-IR spectra are given in Table 2. The sharp OH band at 3643–3644 cm^{-1} is related to the presence of lime. This band appears in the BB (strong) and the FAS, but is not observed in most of the AC samples. The main CO_3 band of calcite [16] is strong in the AC (similar to that of the FED) and weak in the BB and FAS, indicating that further decarbonation to lime occurred in the latter. This band is slightly asymmetric and located above 1425 cm^{-1} in the AC (similar to that of the FED) indicating that in the AC, most of the calcite is original. On the other hand, in most of the BB and in the FAS, this band is strongly asymmetric and located at about 1415 cm^{-1}. It seems that these spectral characteristics are typical of initial recarbonated calcite.

Table 2 Frequencies (cm^{-1}) and relative intensities (RI) of the principal vibrations of OH in lime, CO_3 in calcite, SO_4 in anhydrite and SiO in meta-clay and amorphous Ca-silicates in FT-IR spectra of the AC, FAS and BB ashes produced from organically-rich FED

Samples	Lime		Calcite		Anhydrite		Meta-clay		Amorphous Ca-silicates	
	cm^{-1}	RI	cm^{-1}	RI	cm^{-1}	RI	cm^{-1}	RI	cm^{-1}	RI
AC-I	–		1427	100	1159	29	1041	37	965^{sh}	27
AC-II	–		1428	100	1161	35	1039	32	961	28
AC-8	–		1432	100	1162	62	1041	45	964	41
ACB-117690	–		1426	100	1162	63	1038	47	963	51
ACB-1/3/90	–		1428	100	1161	58	1037	39	963	42
FAS-2	3644	26	1416	59	1151	100	1044	63	923	60
FAS-3	3644	26	1415	56	1152	100	1046	58	926	55
FAS-4	3644	31	1414	49	1150	100	1046	52	918	49
FAS-10	3644	18	1414	46	1149	100	1045	50	921	47
FAS-11	3643	14	1413	44	1149	100	1044	49	922	45
BB-2	3643	75	1515	74	1152	100	1043	74	919	70
BB-4	3643	95	1416	70	1152	100	1043	61	917	71
BB-5	3643	100	1417	72	1151	95	1044	55	922	40
BB-7	3643	100	1421	69	1153	77	1049	62	920	53
BB-10	3643	100	1420	69	1152	82	1045	63	917	54

^{sh}=shoulder

Curve-fitted FT-IR spectra in the range 1750–1250 cm^{-1} of the FED and the three ashes are shown in Fig. 3. The curve fitting data is depicted in Table 3. In the spectra of the FED, the main CO_3 band is fitted with two strong components at about 1470 and 1425 cm^{-1} and a weak component at about 1395 cm^{-1}. On the other hand, in the BB and FAS, this band is fitted with four components at about 1510, 1445, 1425 and 1410 cm^{-1}. It seems that the components at about 1470 and 1425 cm^{-1} are characteristic of original calcite, whereas those at about 1445 and 1410 cm^{-1} are typical of recarbonated calcite. In the AC, the components characteristic of original calcite are strong and those typical of recarbonated calcite appear weak, indicating that the calcite is only slightly decarbonated during combustion. This spectral characteristic is useful for distinguishing between natural and recarbonated calcite within oil shale ashes.

The broadening and asymmetry of the main CO_3 band in the spectra of the recarbonated calcite and the appearance of components at about 1445 and 1410 cm^{-1} in the curve-fitted FT-IR spectra are probably connected with the low crystallinity of the recarbonated calcite and the presence of impurities [12]. Iron and magnesium are probably incorporated by thermal diffusion from the combusted materials to the lime and by crystallization of the recarbonated calcite in contact with the fired clay. It

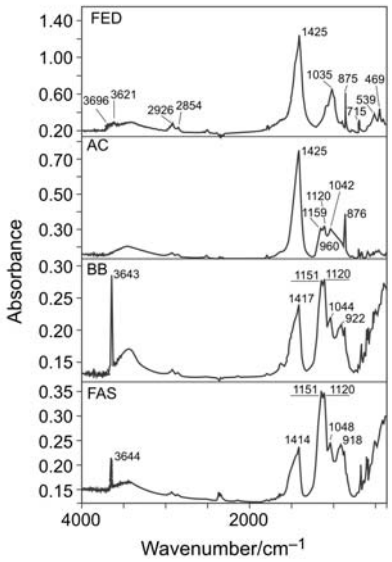

Fig. 2 FT-IR spectra of the FED and the AC, FAS and BB ashes. The spectra demonstrate the presence of lime (3643–3644 cm^{-1}), calcite (1414–1429 cm^{-1}), anhydrite (1150 1159 cm^{-1}), meta-clay (1042–1046 cm^{-1}) and amorphous Ca-silicates (918–965 cm^{-1})

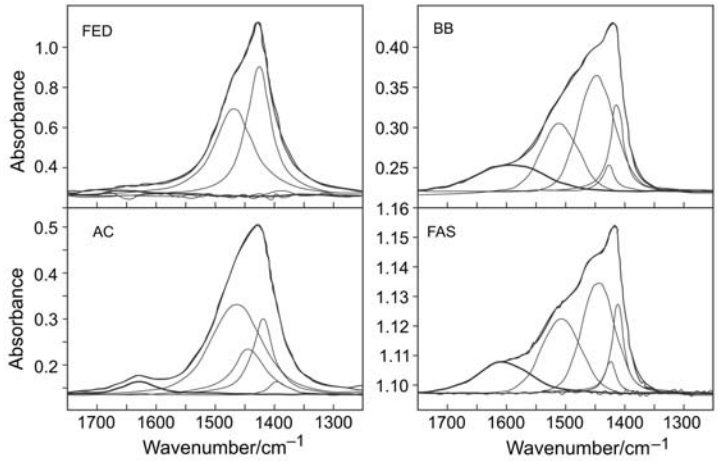

Fig. 3 Curve-fitted FT-IR spectra in the range 1750–1250 cm^{-1} of the FED and the AC, FAS and BB ashes. Components at about 1465 and 1425 cm^{-1} are characteristic of original calcite, whereas those at about 1445 and 1410 cm^{-1} are typical of recarbonated calcite

should be noted that the main CO_3 band is located at about 1415 cm^{-1} in the IR spectra of siderite ($FeCO_3$) and at about 1445 cm^{-1} in the spectra of magnesite ($MgCO_3$) [17]. In addition, amorphous Al-silicates and Ca-Al-silicates are the main component of

Table 3 Frequencies (cm^{-1}), area and width of the main CO_3 band obtained by curve-fitting of the FT-IR spectra of the FED and the AC, FAS and BB ashes produced from organically-rich FED

Samples	Component A			Component B			Component C			Component D		
	cm^{-1}	area	width	cm^{-1}	area	width	cm^{-1}	area	width	cm^{-1}	area	width
FED-6	1470	55.3	77.8	–			1426	53.3	49.1	1390	2.1	40.8
FED-8	1466	86.2	70.9	–			1427	70.8	40.0	1396	0.5	40.8
FED-13	1467	82.7	103	–			1423	46.3	48.4	1393	6.7	43.4
FED-28	1465	45.9	97.9	–			1423	26.5	46.6	1394	3.4	45.1
AC-I	1470	43.2	83.2	1442	15.1	46.8	1421	25.2	38.9	1395	3.5	28.1
AC-II	1473	24.3	93.7	1448	12.8	56.1	1422	16.5	43.0	1395	3.0	31.0
AC-8	1470	25.6	92.5	1443	9.2	46.8	1421	9.5	36.1	1397	2.0	27.2
ACB-117690	1471	38.1	105	1442	10.8	55.9	1420	13.9	43.3	1395	4.4	37.3
ACB-1/3/90	1465	24.2	103	1445	9.1	62.5	1421	10.2	41.5	1396	1.3	28.6
FAS-2	1513	6.1	89.6	1445	6.7	75.6	1424	0.8	25.1	1410	2.8	29.8
FAS-3	1512	5.9	83.6	1445	6.5	75.2	1425	0.5	21.9	1411	3.0	29.0
FAS-4	1512	4.1	83.5	1445	5.4	75.6	1425	0.4	22.5	1411	2.4	28.2
FAS-10	1509	2.9	71.5	1445	5.1	70.9	1427	0.4	17.7	1411	2.4	23.8
FAS-11	1508	2.2	79.9	1446	2.7	67.0	1426	0.3	19.6	1413	1.1	22.9
BB-2	1511	4.5	72.2	1445	11.0	83.3	1428	0.3	16.6	1412	4.2	30.4
BB-4	1512	4.7	81.0	1445	7.5	80.1	1427	0.4	21.2	1412	3.1	30.4
BB-5	1513	3.7	82.2	1445	5.9	80.2	1427	0.4	21.4	1412	2.3	29.7
BB-7	1514	6.1	84.4	1445	7.7	76.8	1427	0.4	17.5	1411	3.7	29.5
BB-10	1510	6.7	74.4	1448	10.8	72.6	1427	1.1	22.8	1413	4.3	27.0

the ashes; Al-silicates are meta-clays and Ca-Al-silicates are to the result of the reaction of some of the lime with the meta-clay. Point chemical analyses in the SEM confirm that all amorphous phases contain significant concentrations of Fe.

Scanning electron microscope

Scanning electron micrographs of AC and FAS ashes are shown in Fig. 4. The AC showed grain shape morphology. 'Holes', probably produced by the expulsion of CO_2, are observed in a large crystal of slightly decarbonated calcite. On the other hand, the FAS and the BB are characterized by an aggregate texture of transformed material. Aggregates of lime accompanied by larger pleosphere-type balls are observed in totally decarbonated calcite. The appearance of the pelospheres in FAS and BB indicate that at least some sintering occurs during ash formation [15].

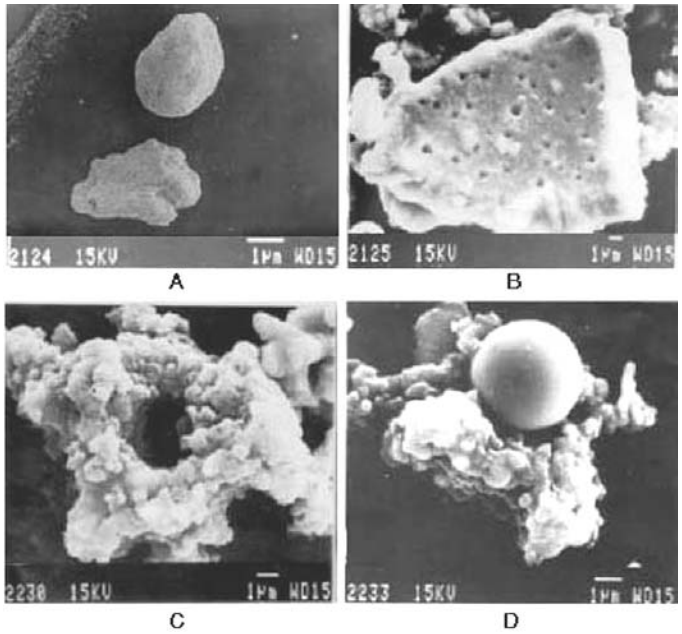

Fig. 4 Scanning electron micrographs of ashes. A – Grain shape morphology of the AC. B – 'Holes' probably produced by the expulsion of CO_2 observed in a large crystal of slightly decarbonated calcite. C – Aggregate texture of transformed material of the FAS. D – Aggregates of lime accompanied by larger pleosphere-type balls observed in totally decarbonated calcite

Isotope analysis

Table 4 summarizes the isotopic analysis data of C and O. The results of the isotopic analyses enable (when the raw material is known) semi-quantitative results of the concentration of the original and the recarbonated calcite [15]. As a rule, both types

of calcite occur in almost all of the analyzed samples. The results are compared with an analysis of the calcareous raw oil shale [18, 19]. The very high negative $\delta^{13}C$ values of calcite from FAS and from some BB (–17.5 and –20.3‰), compared to the $\delta^{13}C$ values of calcite from the FED (–0.3‰), can be explained only by assuming recarbonation of lime with CO_2 originating from the combustion of the organic matter of the raw oil shale (–30.4 to –26.6‰). Thus, the initial recarbonated calcite is formed in the ashes during cooling when in contact with the boiler environment. The observation that some calcite is recarbonated during cooling is supported by DTA experiments [2]. The small changes in $\delta^{13}C$ values (<2‰) produced by heat treatment [20] cannot explain the large differences in $\delta^{13}C$ values of the recarbonated calcite. On the other hand, the $\delta^{13}C$ values of calcite from AC (–5.72‰) are only slightly lower than those of the inorganic calcite of the raw oil shale, indicating that only small part of the calcite is recarbonated and most of it is unchanged original calcite.

Table 4 Comparison of C and O isotopic analyses from the raw oil shale, AC, FAS and BB ashes and atmospheric CO_2

Samples	$\delta^{13}C$‰ PDB	$\delta^{18}O$‰ PDB
Calcite, Bulk Oil Shale B. [18]	–1.96 to –0.21	–4.74 to –1.53
Calcite, Skeletal Oil Shale [19]	–2.5 to –1.6	–3 to –1
Calcite, Diagenetic Oil Shale [19]	–10 to –1.5	–9.5 to –2.5
FED 260499	–0.3±0.01	–0.6±0.01
Calcite, AC 18699	–5.72±0.01	5.07±0.01
Calcite, FAS 18699	–17.5±0.01	–6.33±0.01
Calcite, BB 290792	–20.3±0.01	–10.2±0.01
Organic matter, Bulk Oil Shale [18]	–30.4 to –26.6	–
Atmospheric CO_2	–7	10

Conclusions

The present study shows that the use of XRD, FT-IR, SEM and isotopic analysis methods allows for distinguishing between natural and recarbonated calcite in oil shale ashes. At least part of the calcite is decarbonated during the short residence time in the PAMA's fluidized bed. Initial recarbonated calcite is formed in the ashes during cooling, when in contact with the boiler environment. FAS and BB, which can be compared to fly ash in coal power plants [21], contain more recarbonated calcite than AC, which is comparable to bottom ash in coal power plants. This observation can be explained by the large grains of the AC, which do not reach the highest temperature area, and thus most of the original calcite does not decompose.

Estimation the concentrations of free lime and recarbonated calcite in the ash enables choosing the optimum FED chemical composition to reduce the production of lime during combustion. This allows the use of a greater range of oil shales, thus both reducing mining expenses and obtaining more energy from the combustion.

* * *

We thank PAMA, the Belfer Foundation and The Open University of Israel Research Fund for their financial support. We also thank Dr. T. Minster (Geological Survey of Israel) and A. Wohlfart and S. Cohen (PAMA) for their help in choosing the samples. We are grateful to Dr. R. Calvo and Dr. B. Shilman (Geological Survey of Israel) for carrying out the isotope analyses and M. Dvorachek for his help with the SEM work.

References

1 R. C. Mackenzie, Differential Thermal Analysis, Vols 1, 2, Academic Press, London 1970, 1972.
2 Y. Deutsch and L. Heller-Kallai, Thermochim. Acta, 182 (1991) 77.
3 S. Shoval, M. Gaft, P. Beck and Y. Kirsh, J. Thermal Anal., 40 (1993) 263.
4 L. Heller-Kallai, I. Miloslavski and Z. Aizenshtat, Naturwissenschaften, 73 (1986) 615.
5 L. Heller-Kallai, I. Miloslavski and Z. Aizenshtat, Clay Minerals, 22 (1987) 339.
6 R. C. Mackenzie and A. A. Rahman, Thermochim. Acta, 121 (1987) 51.
7 S. Shoval, Thermochim. Acta, 135 (1988) 243.
8 Kingery, Journal of field archaeology, 15 (1988) 219.
9 M. Maciejewski and A. Reller, Thermochim. Acta, 142 (1989) 175.
10 M. Maggetti, H. Westley and J. S. Olin, In Archaeological Chemistry, American Chemical Society, (1984) 151.
11 M. P. Riccardi, B. Messiga and P. Duminuco, Appl. Clay Sci., 15 (1999) 393.
12 S. Shoval, J. Thermal Anal., 42 (1994) 175.
13 T. Minster, O. Yoffe, Y. Nathan and A. Flexer, Israel Journal of Earth Science, 46 (1997) 41.
14 O. Yoffe, Unpublished Ph.D. Thesis, Hebrew University of Jerusalem, 1997, p. 91 (in Hebrew, English abstract).
15 O. Yoffe, Y. Nathan, A. Wolfarth, S. Cohen and S. Shoval, Fuel, 81 (2002) 1101.
16 W. B. White, The carbonate minerals. pp. 227–284 in: The Infrared Spectra of Minerals. V. C. Farmer, Ed. Monograph 4, Mineralogical Society, London 1974.
17 H. W. van der Marel and H. Beutelspacher, 'Atlas of Infrared Spectroscopy of Clay Minerals and their Admixtures', Elsevier, Amsterdam 1976, p. 57.
18 B. Spiro, Unpublished Ph.D. Thesis, Hebrew University of Jerusalem, 1980, p. 152. (in Hebrew, English abstract).
19 E. Sass, A. Bein and A. Almogi-Labin, Geology, 19 (1991) 839.
20 K. M. Thomas, F. Dillon, S. Bottrell, P. K. K. Louie and K. D. Bartle, Carbon, 31(1993) 273.
21 Y. Nathan, M. Dvorachek, I. Pelly and U. Mimran, Fuel, 78 (1999) 205.